



Dissolution Enhancement of Ketoconazole by Melt Granulation Co-Processing

Abigail Garcia-Radilla¹ , Mariana Ortiz-Reynoso^{1*} , Gabriel Cuevas² , Edna T. Alcantara-Fierro¹
and Jonnathan G. Santillán-Benitez³

¹Laboratory of Pharmacy, Faculty of Chemistry, Autonomous University of Mexico State, Toluca, State of Mexico, Mexico, 50120.

²Laboratory of Natural Products Chemistry, Institute of Chemistry, National Autonomous University of Mexico, Mexico City, Mexico, 04510.

³Laboratory of Molecular Biology, Faculty of Chemistry, Autonomous University of Mexico State, Toluca, State of Mexico, Mexico, 50120.

*mortizr@uaemex.mx (Corresponding Author)

ARTICLE INFORMATION

Received: 02 July, 2024

Revised: 09 August, 2024

Accepted: 20 September, 2024

Published Online: 20 November, 2024

Keywords:

Melt granulation, Dissolution rate, High-shear mixer, Co-processed ketoconazole

ABSTRACT

Background: Melt granulation (MG) is a simple operation involving a uniform mixture of active ingredients with a melted polymeric carrier. However, this process can also enhance a drug's biopharmaceutical properties by augmenting its dissolution rate and, thus, its absorption.

Purpose: By applying MG technology, current research focuses on developing co-processed ketoconazole with a higher aqueous dissolution rate than its pure form.

Methods: A measure of how the type and proportion of polymeric carriers affect the crystallinity and dissolution rate of co-processed ketoconazole materials was performed. MG prepared materials in a high-shear mixer using co-povidone (Kollidon®) VA 64, HPMCAS HF as polymeric carriers, PEG 1450 (Kollisolv®) and triethyl citrate as plasticizers.

Results: The co-processed ketoconazole materials exhibited miscibility in the polymeric systems, as indicated by the reduction in the enthalpy of fusion. Drug crystallinity was significantly reduced in the HPMCAS HF polymeric system, confirmed by XRPD and ATR-FTIR studies. The dissolution rate was enhanced by using a higher drug concentration in a co-povidone VA 64 environment; contrarily, for HPMCAS HF, a higher drug dilution was observed to favor the dissolution rate.

Conclusions: MG is a handy, low-cost technology that develops dissolution-enhanced co-processed active pharmaceutical ingredients, spotting specific carrier-drug interactions. MG yields scalable, proven processes, raising interest in its applications in optimizing drug therapeutic efficacy. Ultimately, this technology for dissolution enhancement could bring lower-cost, high-efficiency drugs to improve patients' quality of life.



DOI: [10.15415/jptrm.2024.122001](https://doi.org/10.15415/jptrm.2024.122001)

1. Introduction

Most solid oral active pharmaceutical molecules going under developmental phases have low aqueous solubility, impairing drug absorption, thus leading to low plasma concentrations that compromise the therapeutic effect. There are several technologies available to address the low solubility of drugs. Powder granulation is a technique that has been used for decades in the pharmaceutical industry to enhance the compression and flow properties of drugs when manufacturing hard-gelatin capsules and tablets and presents two classic alternatives: the wet route (using a solvent to activate the binder) (Singh *et al.*, 2022) and the dry route (applying a mechanical force to bind the particles together) (Jaspers *et al.*, 2022). Solid dispersion technologies have also been widely studied (Jadav & Paradkar, 2020).

Recently, a third variant of granulation, known as melting granulation (MG), emerged. This method has been successfully used to modify active pharmaceutical ingredients (API), improving their bioavailability, which is possible by increasing drug absorption by enhancing the dissolution rate. MG's development of pharmaceutical products may involve manufacturing higher-dose drugs in lesser volumes, resulting in single-step manufacturing. This allows low-cost processes and reduces energy consumption (Steffens *et al.*, 2020; Jadav & Paradkar, 2020). MG increases the size of primary particles when using a melting carrier that binds up API particles when heat is generated. The process temperature must be below the drug's melting temperature (T_m) but above the T_m or glass transition temperature (T_g) of the polymeric carrier (Sarpal *et al.*, 2020). Melt granulation is usually performed in high-shear mixers (HSM). The process

begins by physically mixing the drug and polymer with the continuous motion of the impeller at a speed under 1500 rpm. This results in an even distribution of the drug within the polymeric carrier, yielding a homogeneously dispersed solid mixture after cooling down the materials. The melting process is carried out with two sources of energy: the temperature rise generated by the high-shear motion and a heating jacket that reaches temperatures between 50-90 °C. The mixing system comprises a chopper to prevent excessive agglomeration of the product under 3000 rpm speeds. Both mechanisms of the mixing system, impeller, and chopper, induce particle collisions and can generate enough kinetic energy to break down the crystalline structure of the drug, thus increasing molecular interactions (Steffens *et al.*, 2020).

The melt granulation mechanism occurs in three steps. First, the polymeric carrier reaches a vitreous or melting state, starting a granular nucleation phase in which small clusters of solid particles form within the polymeric carrier. As solid nuclei build up, smaller particles fuse in to give birth to larger granules through the coalescence of adjacent nuclei. Eventually, the attractive forces among the particles exceed the repulsive forces, generating denser and more resistant granules and moving to a consolidation phase. Following coalescence and consolidation, granules may grow further as more individual particles join in the existing structure or through the agglomeration of smaller granules to form larger ones. Finally, shear forces break off granules, leading to the fragmentation or disintegration of larger granules into smaller ones (Bouffard *et al.*, 2012); this phase renders size uniformity to the granules.

An advantage of HSM is that this equipment is available in a fair sum of generic drug plants and pilot-scale laboratories. This may pose an opportunity to develop new applications out of well-known technology, avoiding significant investments (Garcia *et al.*, 2023). A disadvantage of MG in HSM is that the equipment operates at low temperatures, limiting the variety of available polymeric carriers. To overcome this weakness, ternary systems have emerged involving the addition of plasticizers and surfactants (Sarpal *et al.*, 2020). Plasticizers conveniently reduce the polymer carrier's glass transition temperature (T_g), consequently reducing the melting temperatures required.

On the other hand, surfactants help reduce the particle size, thus increasing their relative surface area, yielding higher drug solubility rates. MG's immediate-release drug delivery systems use hydrophilic binders to enhance poorly soluble drugs' solubility and dissolution rate. In contrast, lipophilic binders are preferred to develop controlled-release systems (Steffens *et al.*, 2020).

Several studies have concentrated on enhancing the dissolution rate of different drugs, but the number narrows

down if HSM is used in the process. The following studies have yielded favorable outcomes when attempting to augment the dissolution rate through melt granulation techniques in HSM. Crowley *et al.* (2000) achieved a 90% dissolution of propranolol in just 2 min (compared to the 25 min required by the pure drug). Perissutti *et al.* (2003) modified the rheological properties of carbamazepine by adding crospovidone, speeding the dissolution rate up to 3.7 times for the pure molecule. Ye *et al.* (2007) also enhanced the dissolution rate of itraconazole by manufacturing pellets from solid dispersions; these dissolved more than 70% of the drug within 45 min (whereas pure itraconazole dissolved less than 1%). These studies have consistently demonstrated that solid dispersions can significantly enhance the dissolution of different drugs, an essential aspect of their therapeutic efficacy (Garcia *et al.*, 2023). We hypothesize that co-processed ketoconazole manufactured by an MG process can enhance the drug's vitro dissolution rate.

Ketoconazole (KTZ) was the first synthetic lipophilic azole antifungal oral drug showing a broad-spectrum approved by the Food and Drug Administration (FDA) in 1981 (De Almeida *et al.*, 2019). It is used in the treatment of superficial or systemic fungal infections, in type 2 diabetes, cushing's syndrome, and hirsutism, and as a second-line indication for the treatment of advanced prostate cancer (de Almeida *et al.*, 2019; European Medicines Agency (EMA), 2014). This active pharmaceutical ingredient (API) has a melting point of 148 - 152 °C and is a weak base with values $pK_{a1} = 6.51$ (imidazole ring); $pK_{a2} = 2.94$ (piperazine ring) (Figure 1) (Sarpal *et al.*, 2020), resulting in pH-dependent solubility (indeed, it is just soluble under highly acidic conditions). The solubility in water is 17 µg/ml, impacting the drug absorption when administered orally. The low solubility of this drug is attributed to its crystalline hydrophobic structure; however, the molecule has a high permeability in the gastrointestinal tract (de Almeida *et al.*, 2019). KTZ belongs to Class II of the Biopharmaceutical Classification System of Drugs (BCS).

This study aims to develop co-processed ketoconazole with a higher aqueous dissolution rate than pure ketoconazole by a melt granulation method carried out in a high-shear mixer and to describe the effect of the type and proportion of polymeric carriers on the degree of crystallinity and drug dissolution rate. The quality of the co-processed was determined through the following output parameters: for the characterization of the solid state of the KTZ co-processes were carried out to differential scanning calorimetry (DSC) tests, percent crystallinity, X-ray diffraction (XRD) and microscopy with computerized image analysis. Molecular identity and evaluation of intermolecular interactions of ketoconazole co-processes were verified by infrared spectroscopy (IR).

The physicochemical analysis of drug release quantification concerning time was performed by in vitro dissolution in an aqueous medium. Co-povidone VA 64 (Kollidon®) and HPMCAS HF were selected as polymeric carriers. Both are amorphous and hydrophilic, described in the scientific literature as enhancers for dissolution rate in formulations manufactured by the hot melt extrusion (HME) technique (Vaka *et al.*, 2014). However, these polymers have not been studied in MG processes. These carriers have also not

been studied in combination with polyethylene glycol and triethyl citrate plasticizers to know their effect on reducing the processing temperature.

By developing a co-processed ketoconazole with a higher aqueous dissolution rate than pure ketoconazole by a melt granulation method carried out in a high-shear mixer, we can prove that low-cost readily available technologies can be very helpful in developing improved raw materials, including active pharmaceutical ingredients.

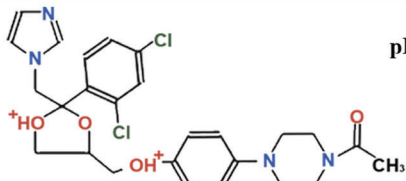
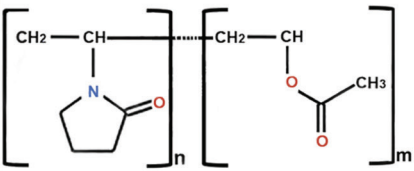
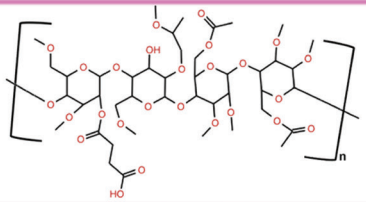
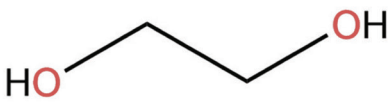
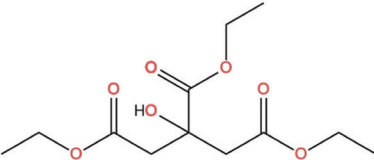
APY	Ketoconazole		MW (g/mol) = 531.44 pKa = 6.5 (imidazole group); 2.9 (piperazine group) Tm (°C) = 148 - 152 Tg (°C) = 42.1 Td (°C) = 221.3 Aqueous Solubility = 17 ug/ml Physical form = Crystalline
	POLYMERIC CARRIERS	Copovidone (Kollidon® VA64/Plasdone™ S-630)	
Hydroxy propyl methyl cellulose acetate succinate (HPMCAS)			MW (g/mol) = 50, 000 Tg °C = 122 Td °C = 276 Aqueous Solubility (pH) = 6.8 Physical form = Amorphous Hygroscopicity = High
PLASTICIZERS		Kollisol® PEG 1450	
	Triethyl citrate		MW (g/mol) = 276.28 Tg °C = -75 Aqueous Solubility = moderate

Figure 1: Physicochemical properties of the raw materials used in this research work.

Source: Own elaboration with information from Garcia *et al.* (2024)

2. Methods

2.1. Description of Materials

Ketoconazole (Piramal Enterprises Ltd., batch: KET/M-23117) was used as a model drug, copovidone VA 64 (Kollidon®, BASF Pharma Co., batch: 56741056P0) y polyethylene glycol (PEG) 1450 (Kollisolv®, BASF Pharma Co., batch: GNF00421B); HPMCAS HF (AQOAT AS-HF®, Shin Etsu Chemical Co. batch: 65G-810002) donated by Ashland; and triethyl citrate (TEC) donated by Sigma-Aldrich (Batch: W308302-1KG-K).

2.2. Methodological Approach

2.2.1. Differential Scanning Calorimetry (DSC)

The calorimetric analysis by DSC was conducted using an instrument uploaded with STARE software (Mettler Toledo, DSC-3). An analytical balance (Ohaus, Pioneer PA214) weighed the samples. Each sample, weighing 12-15 mg, was placed in a 40 µl aluminum crucible with pierced lids and hermetically sealed using a press. The heating rate was at 3°K/min within a temperature range of 25-200 °C in a nitrogen atmosphere with a 10 ml/min flow rate. The temperature values for glass transition (T_g), melting (T_m), and enthalpy of fusion were recorded. Additionally, the percentage of crystallinity was calculated using Equation 1 to relate the result with the miscibility among carrier polymers (Chan *et al.*, 2015), plasticizers, and pure drugs.

$$\% \text{crystallinity} = \frac{\Delta H_f \text{ physical mixture}}{\Delta H_f \text{ Pure KTZ}} \times 100 \quad (1)$$

Where (ΔH_f): Fusion Enthalpy

This quotient indicates the reduction between the interactions in the KTZ crystal lattice, normalizing the values concerning the pure drug as a percentage relative to the initial crystallinity. The measurements were repeated twice.

2.2.2. Melt Granulation in a High-Shear Mixer

Twelve batches of ternary mixtures (Polymer + plasticizer: Drug) were manufactured with each polymer: copovidone VA 64 and HPMCAS HF, adding plasticizers PEG 1450 and TEC, respectively (Table 1) in a 2 L HSM (Sainty Co, SMG2-6) equipped with a chopper, a three-blade stainless steel impeller, comprising a ceramic and stainless-steel electric heating resistance and a thermocouple for temperature control. The batch size was 100 g. The kneading time was adjusted for each batch according to each polymer's T_g (previously obtained by calorimetric analysis) and defined as the time required to exceed 20 °C the T_g of each polymeric carrier (Vaka *et al.*, 2014). Temperatures were recorded in each test. The granules were poured into a stainless-steel container, cooled to room temperature for 30 min, and stored in plastic bottles with lids for subsequent analysis. Preliminary microscale tests (not shown here) optimized the amount of plasticizer used, the appropriate amount of polymeric carrier, and the melting temperature at which the process was undertaken (García *et al.*, 2024), so it was decided to divide it into three individualized steps for each polymer in the manufacturing process (Table 2). Physical mixtures were tested as a negative control to correlate the results with the granulation process, not the simple mixing of components.

Table 1: Composition of the Different Formulations of Co-Processed Ketoconazole

Formulation	Proportion Polymer+%Plasticizers:Drug	Polymer (g)	Plasticizers (g)	Drug (g)
PM-K	50 % Kollidon® VA 64+10%PEG: 50 % KTZ	45	5	50
F1	33 % Kollidon® VA 64+10%PEG: 67 % KTZ	29.7	3.3	67
F2	25 % Kollidon® VA 64+10%PEG: 75 % KTZ	22.5	2.5	75
PM-H	50 % HPMCAS HF+20%TEC: 50 % KTZ	40	10	50
F3	33 % HPMCAS HF+20%TEC: 67 % KTZ	26.4	6.6	67
F4	60 % HPMCAS HF+20%TEC: 40 % KTZ	48	12	40
PM: Physical mixtures F: Formula				

Table 2: Steps in the Manufacturing of Co-Processed Ketoconazole

Procedure			
Polymer	Step 1: Premixed	Step 2: Melt Granulation	Step 3: Cooling
Kollidon® VA 64	The three components were placed in the HSM, Polymer + 10% Plasticizer: KTZ; the airflow ¹ was turned on, and the impeller was at 1000 rpm for 5 min.	While stirring, the electrical resistance was turned on. When a temperature of 70 °C was reached, the chopper was turned on at 1000 rpm for 3 minutes.	The electric resistance was turned off once the temperature reached 75°C. The impeller speed was reduced to 50 rpm and turned off when the mass temperature descended to 50 °C.
HPMCAS HF	The polymer was placed in the HSM; plasticizer was added using the peristaltic pump at 1 rpm at a 1 bar pressure; airflow ¹ was turned on; the impeller was on for 5 min, at 1000 rpm.	While stirring, the electrical resistance was turned on. When a temperature of 40 °C was reached, the impeller speed was decreased to 50 rpm, and KTZ was added. The impeller speed was again increased to 1000 rpm, and as the temperature reached 70 °C, the chopper was turned on for 3 min at 1000 rpm ² .	
¹ Airflow unchanged throughout the process. ² Chopper speeds remained constant for all tests.			

Rask *et al.* (2016) found that to achieve a cost-effective formulation as an administration system, the drug load must be more significant than 20%. This was why formulations of co-processed having 40, 50, 67, and 75% of drug load were considered in the current study.

2.2.3. Powder X-Ray Diffraction (PXRD)

A spectrometer (Bruker D8 Advance) with Bragg-Bretano geometry was used for powder X-ray diffraction (PXRD) measurements. Monochromatic radiation was generated from a CuK α 1 ($\lambda = 1.5405 \text{ \AA}$) source and Linxeye detector under a current of 25 mA and a voltage of 30 kV. The scanning speed was 0.03°/s, ranging from 5° to 80° (2 θ).

2.2.4. Attenuated Total Reflectance – Fourier Transform Infrared (ATR-FTIR) Spectroscopy

The Nicolet IS50 FTIR instrument, equipped with a diamond ATR crystal, was used to acquire the ATR-IR (Attenuated Total Reflectance) spectra. The solid-state sample was placed onto the crystal. The sidebands, caused by the different penetration depths of the infrared light beam into the sample, were corrected using the standard software that was equipped.

2.2.5. In Vitro Dissolution Tests

The dissolution test was duplicated using a dissolution USP Apparatus I “baskets” (AT7-Sotax, Switzerland). Each basket contained 30 mg of ketoconazole on filter paper in 900 ml of 0.1 N hydrochloric acid (pH: 1.2) and phosphate buffer (pH:

6.8) at $37 \pm 0.5 \text{ }^\circ\text{C}$. Copovidone VA 64 was evaluated in HCl pH 1.2 to simulate the gastric environment, while HPMCAS HF co-processed was evaluated in phosphate buffer pH 6.8 to simulate the intestinal environment. The dissolution time and pH for dissolution tests were selected based on the characteristics of the polymers, simulating the conditions to which the drug would be exposed in the gastrointestinal tract. Copovidone VA 64 is reported to be hydrophilic; therefore, one hour is sufficient for its dissolution. On the other hand, the dissolution of HPMCAS HF is dependent on the amount of polymer, having a diffusion-controlled effect, with an optimal pH of 6.8 (Auch *et al.*, 2020; Freichel & Lippold, 2001; Nair *et al.*, 2020).

Samples were taken in 5 ml aliquots at 5, 10, 15, 20, 30, 45, and 60 min for the HCl test. The phosphate buffer's time intervals were 5, 10, 20, 30, 40, 50, 60, 80, 100, 120, 150 and 180 min, replacing the dissolution medium. The samples were analyzed using a UV-Vis spectrometer (Thermo Scientific, Genesys 10S) at a wavelength of 223 nm (0.1 N HCl) and 208 nm (phosphate buffer, pH 6.8). The drug concentration was obtained by interpolating the absorbance data into the Equation straight from a standard curve. The dissolution rate was calculated as the slope of the line resulting from the plot of concentration versus time.

2.2.6. Statistical Analysis

One-way analysis of variance (ANOVA) was applied to determine if there was a significant difference ($p < 0.05$) existed among the formulations. Tukey's multiple comparison test

was then performed. A linear regression was conducted to determine the dissolution rate.

The dissolution test results were presented as the mean \pm standard error of the mean (SEM) for two replicates (n=3). All other analyses were performed on two experimental samples (n=2). Statistical analysis was done using Prism 8.0.1 software (Graphpad Software, Inc.).

3. Results and Analysis

3.1. Differential Scanning Calorimetry

Figure 2A illustrates the thermal event curves obtained by DSC for different raw materials. The obtained glass

transition temperatures were 94.75 °C for co-povidone VA 64 and 123.75 °C for HPMCAS HF. In the case of KTZ, the endothermic peak was observed at 151.24 °C, while the plasticizer PEG 1450 exhibited a signal at 49.54 °C, corresponding to their respective T_m values. Figure 2B shows the endothermic behavior of the co-processed, demonstrating a decrease in the T_m of KTZ in the presence of each polymer as a meltable carrier. Specifically, co-processed F1 and F2 exhibited T_m values of 147.32 °C and 150.08 °C, with ΔH_f of 55.55 J/g and 66.61 J/g, respectively (red box). Likewise, F3 co-processes presented T_m of 146.65 °C and ΔH_f of 72.41 J/g, while F4 showed a significant decrease in the enthalpy of fusion (ΔH_f : 15.79 J/g, T_m : 135.95 °C) (red box)

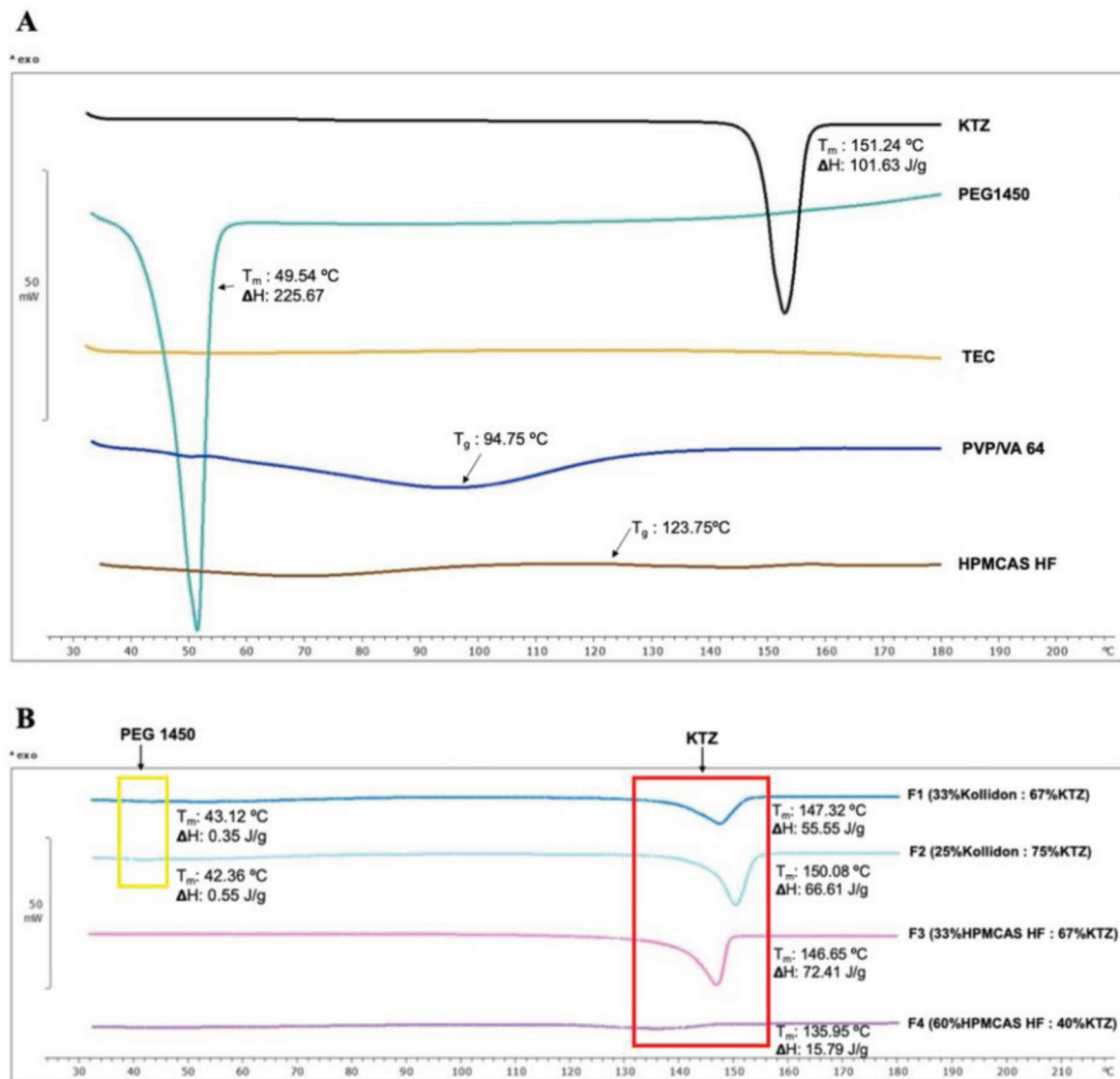


Figure 2: DSC thermograms. (A: Thermal events of raw materials; B: Thermal events of KTZ co-processed with co-povidone VA 64 and HPMCAS HF in different proportions)

All co-processed samples demonstrated a shift in the T_m of KTZ, indicating good miscibility in the drug-polymer-plasticizer system and suggesting the formation of a single-phase mixture. According to Medarević *et al.* (2019) an increased amount of polymeric carrier causes a shift/depression of the fusion enthalpy and an amplitude change in the fusion peak. These findings correspond to the results obtained for the HPMCAS HF co-processed systems, which indicate that a higher proportion of this polymer leads to a decrease in the intensity peak and a significant shift of the endothermic peak of KTZ. Thus, confirming Medarević *et al.* (2019) outcomes: a higher amount of polymer enables the drug to be dispersed/dissolved at a molecular level within the polymeric lattice because this leads to a physical modification of the drug's crystalline structure, resulting in an increased dissolution rate. If the drug and polymer are miscible, they can form a homogeneous solid solution, probably leading to a decrease in the drug melting temperature, depending on

the nature of the interactions among the molecules. The formation of hydrogen bonds, dipole-dipole forces, or other intermolecular interactions between the drug and the polymer can influence the energy required to break these interactions down during the melting process.

The percentage crystallinity calculations, as shown in Figure 3, revealed a reduction in the crystalline nature of the co-processed samples with co-povidone VA 64 and HPMCAS HF carriers compared to pure KTZ ($p < 0.0001$). Significant differences were observed in the evaluated proportions of each polymer, highlighting the decrease in the degree of crystallinity in F1 compared to F2 ($p = 0.0176$) and F3 ($p = 0.0115$). However, F4 co-processed exhibited the lowest degree of crystallinity, approximately 86.25% lower than pure KTZ. This difference was significant when compared to all other manufactured co-processed ($p < 0.0001$). These results indicate a more significant molecular-level interaction between the drug and carriers, as evidenced by the reduction in crystallinity.

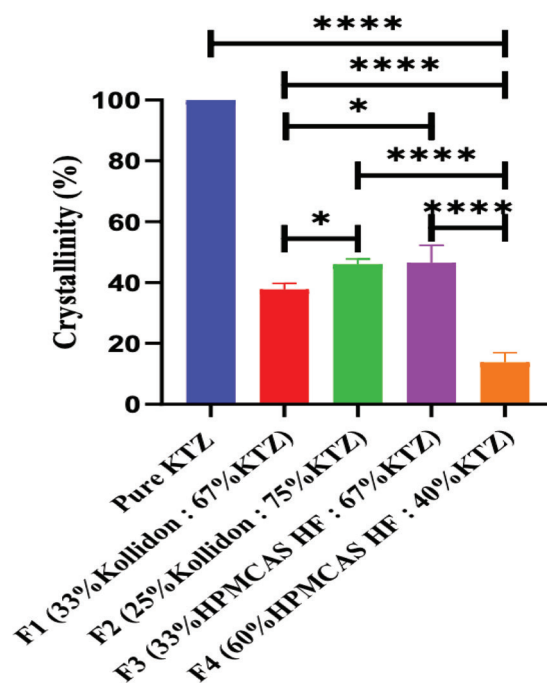


Figure 3: Crystallinity Percentage of KTZ Co-Processing.

Results are presented as mean and SEM ($n=2$). One-way ANOVA followed by Tukey's post hoc test. * $p=0.0176$, 0.0115 ; **** $p < 0.0001$.

3.2. Powder X-Ray Diffraction (PXRD)

The PXRD results reveal significant findings. Figure 4A shows the characteristic diffraction pattern of the crystalline state of KTZ and PEG 1450. The peaks show higher intensity in the 2θ range between 5 and 30 for both components. In the case of co-processed co-povidone VA 64 in various

proportions, an incipient reduction in the intensity of KTZ peaks is observed.

A similar trend is observed in formulation F3 (made with the carrier HPMCAS), indicating a slight decrease in the crystallinity degree of KTZ (Figure 4B). For F4, a significant reduction in peak intensity is observed, and some characteristic signs of the crystalline nature of KTZ even

disappear (Figure 4A). This suggests that in F4 (with a KTZ content of 40%), the drug partially adopts an amorphous form, and the remaining KTZ crystals are smaller. The degree of crystallinity was measured using two distinct techniques: DSC and PXRD. The resulting data from both methods were consistent, supporting the percentage crystallinity

analysis conducted via DSC, as illustrated in Figure 3. Based on these results, it can be inferred that a solid dispersion of glass suspension was obtained. This indicates that the drug could be “pre-dissolved” or at least finely dispersed as crystalline particles in the polymeric carrier, theoretically enhancing the dissolution rate (Yazdani *et al.*, 2020).

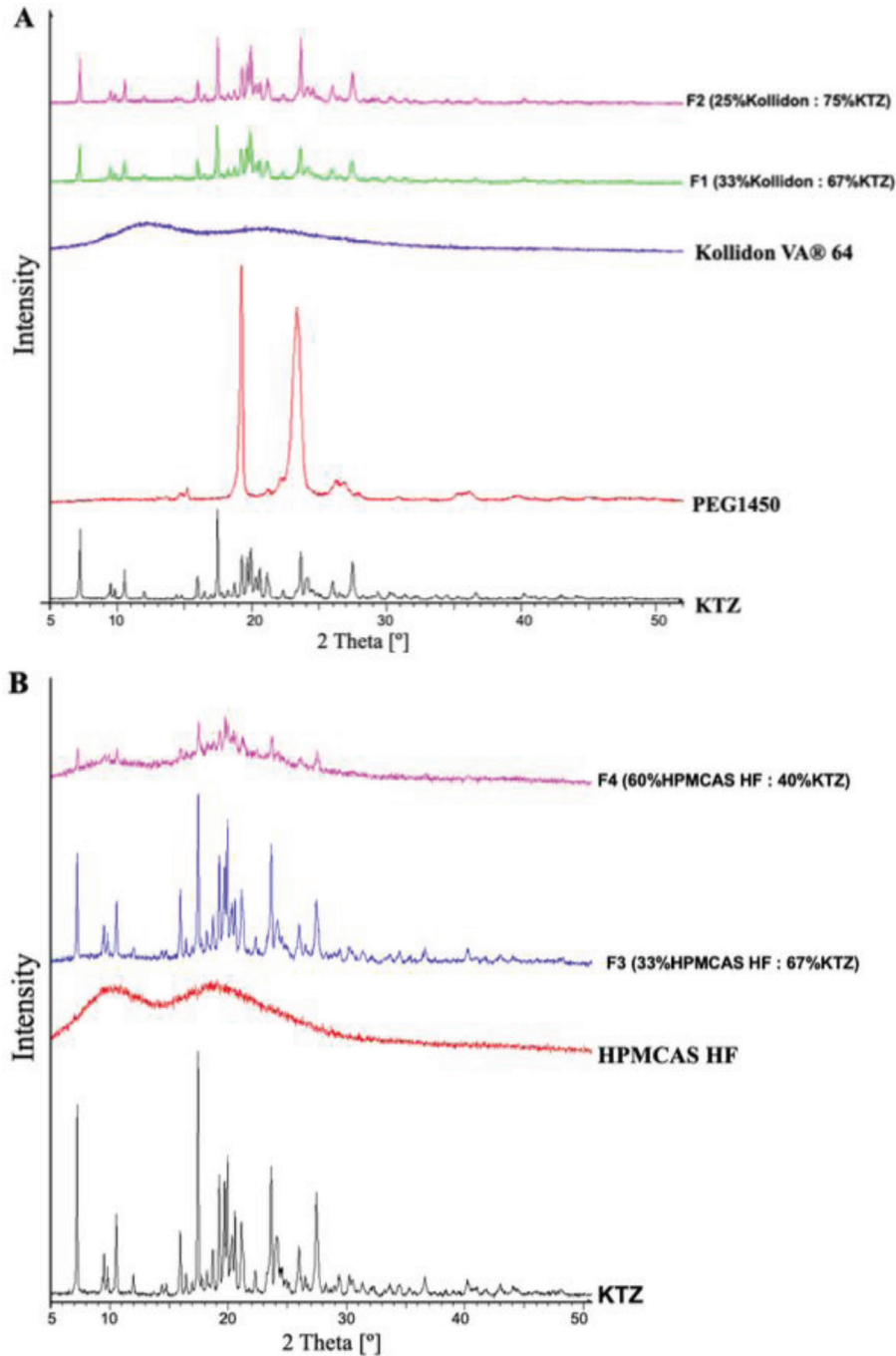


Figure 4: Powder X-ray diffraction (PXRD) diffractogram. (A: Diffraction pattern of raw materials and co-processed based on co-povidone VA 64; B: Diffraction pattern of raw materials and co-processed based on HPMCAS HF)

3.3. ATR-FTIR Spectroscopy

The infra-red IR spectrum (ATR-FTIR) obtained from KTZ (Figure 5) displays bands that are characteristic of aromatic components (around 3119 cm^{-1}) and aliphatic hydrocarbons (2881.80 cm^{-1}). Also, at 1644 cm^{-1} , a carbonyl of the acetamido group appears. At 1510 cm^{-1} , the stretching

C=C of the aromatic rings is shown. A signal attributable to a tertiary amide towards 1243 cm^{-1} was detected, as well as that produced by C-Cl bonds at 813 cm^{-1} , which is complemented by others appearing towards 719 cm^{-1} . On the other hand, polyethylene glycol, which likely contains traces of water, shows signals characteristic of C-O bonds and hydrocarbon signals.

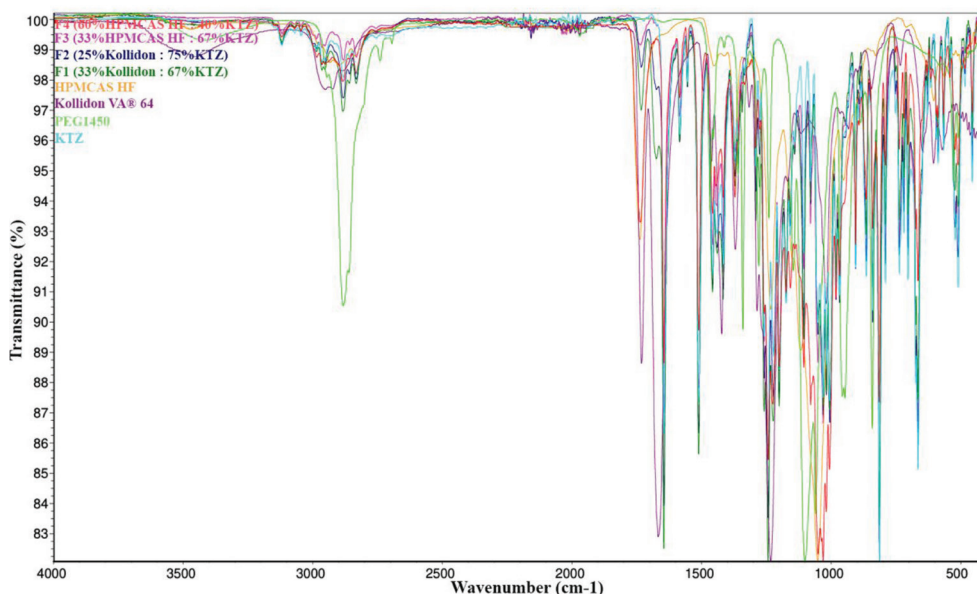


Figure 5: ATR-FTIR Spectra of Raw Materials and Co-Processed KTZ Based on Kollidon VA 64 and HPMCAS HF

The ATR-FTIR of the polymer formed by the polyvinylpyrrolidone/vinyl acetate carrier shows signals characteristic of carbonyl groups. For vinyl acetate, a signal of medium intensity develops at 1730 cm^{-1} , confirming the stretching of the carbonyl of the acetyl group, and at 1665 cm^{-1} , another signal shows for the pyrrolidone carbonyl. At 1232 cm^{-1} , the stretching C-O appears, and around 3445 cm^{-1} , such does one for the O-H stretching, possibly caused by moisture in the analyzed sample, the polymer skeleton, and the substituents. The HPMCAS-HF carrier presents a strong signal at 1051 cm^{-1} , suggesting the C-O stretching. The hydroxyl groups are responsible for the observable signals at 3470 cm^{-1} , while the carbonyl groups of a succinic acid derivative and acetic acid generate the slightly broad signal as shown at 1737 cm^{-1} .

The co-processed samples exhibit absorption bands characteristic of both drug and polymers, albeit with some changes. As seen in the spectrum labeled F1 (33% co-povidone VA 64 and 67% KTZ), the signal of the amide carbonyl group (1644 cm^{-1}) signal remains unchanged. However, there is a substantial decrease in the intensity of the carbonyl signals of the polymeric

carrier. This is accentuated in the spectrum labeled F2 (25% co-povidone VA 64 and 75% KTZ). The decrease in the signals goes beyond just a change in the proportion of the mixture's components. According to Coksu *et al.* (2023), a significant decrease in the intensity of the dominant signals, along with the predominance of drug signals, indicates that the carrier is encapsulated in the drug.

Due to co-povidones' nature, carbonyl groups can be associated with protic solvents through hydrogen bonding. Indeed, this carrier's manufacturer highlights these co-povidones' ability to dissolve in alcohol and water. These carbonyl groups can also participate as acceptors of unshared electron pairs through the $n\text{O} \rightarrow \pi^*\text{C}=\text{O}$ interaction. Both types of interaction are recognized as the strongest weak interactions known. Conversely, ketoconazole is a low-solubility compound lacking hydroxyl groups but possessing acceptors of these. Therefore, a poor association between the heteroatoms of the imidazole and co-povidone can be expected. This contact becomes relevant when atoms donating unshared electron pairs (N, Cl, O) interact with co-povidone's carbonyl groups. Consequently, the involvement of

carbonyl groups in the two most relevant weak interactions will cause elongation of the C=O bond, thus resulting in a decrease in bond strength, thereby modifying the vibration frequency. In a well-studied case of interaction, the carbonyl signal subject to interaction can shift from 1703 cm^{-1} in the free-state to 1693 cm^{-1} in the associated state (Tamez-Fernández *et al.*, 2021).

Of course, the hydrocarbon chain supporting acetate and pyrrolidone can also engage in CH/ π type interactions, which, although less stabilizing, can occur in a greater quantity. Given their additivity, they can result in an energetically significant contribution. The aromatic rings (phenyl and imidazole) can enhance molecular stability (Ramírez-Gualito *et al.*, 2009). Another relevant interaction in supramolecular stabilization is the H-H interaction, which, contrary to a widespread idea, has proven to stabilize in a specific range of distances or is certainly repulsive only at very close distances. Due to the low interaction energy, characterizing and measuring it is highly complicated due to the low interaction energy, but it is undoubtedly an additional interaction that must be considered (Duarte Alaniz *et al.*, 2015).

In the case of the second carrier, HPMCAS HF, the spectrum labeled F3 (33% HPMCAS HF) can be interpreted with the same principle as before, except in this case, it is KTZ that is encapsulated within the carrier, as expected. However, this encapsulation is not observed in the spectrum F4 (60% HPMCAS HF). This is likely attributed to the KTZ groups' capability to accept hydrogen bonds that are present in the second carrier and absent in the first, thus hindering the generation of constructive and stabilizing supramolecular interactions.

3.4. In Vitro Dissolution Tests

All co-processed systems of co-povidone VA 64 demonstrate that two conditions must be met to enhance the dissolution rate: a higher concentration of the active ingredient and a high-shear manufacturing process (high kinetic energy) at elevated temperatures.

However, it's mentioned that the conventional DSC heating process induces the disintegration of drug molecules, and this test could generate a misconception of the solid state of the drug in the polymeric carrier (Medarević *et al.*, 2019). In this regard, in the case of co-povidone VA 64-based co-processed materials, a reduction in the fusion enthalpy was observed, and therefore, from a logical point of view, we would have expected to have an increase in the dissolution rate of KTZ; however, this was not the case as there was no enhance in dissolution in the F1 co-processed system (33% co-povidone VA 64), indicating that the co-processed system has a release profile similar to pure KTZ and the physical mixture

(PM-01) in a 50:50 proportion (figure 6A). These results are consistent with those of PXRD analysis (which showed no modification in the solid state of KTZ) and ATR-FTIR spectroscopy study (which showed no significant changes in absorption bands), indicating a low level of drug-polymer interaction in both drug concentrations (thus preserving the crystalline structure of KTZ). However, the dissolution rate was not negatively affected for the co-processed formula F2 (25% co-povidone VA 64). One possible explanation is that the high hydrophilic nature of the polymer in aqueous media promotes the release of molecules/particles into the solvent. In the F2 co-processed system (25% co-povidone VA 64), the release of KTZ experienced a remarkable 20% increase in the first 5 minutes compared to the pure drug, as shown in Figure 6A. After 60 minutes, the average release reached almost 87%, which is significantly higher than the 74% of the pure drug during the same period. The graph in Figure 6B shows that at $t=30$ minutes, the co-processed formula F2 (25% co-povidone VA 64) shows significant differences compared to pure KTZ ($p=0.0007$), the physical mixture ($p<0.0001$) and the co-processed system F1 ($p=0.0003$). However, at 60 minutes, no significant differences were found between pure KTZ and the co-processed systems, although an increasing trend was observed for the co-processed F2 (25% co-povidone VA 64) when compared to pure KTZ ($p=0.5402$). Significant differences are shown between the co-processed F2 (25 % co-povidone VA 64) and F1 (33 % co-povidone VA 64) ($p=0.0142$) and the physical mixture ($p=0.0102$).

The results of the HPMCAS HF co-processed systems indicate that a higher dilution of the active ingredient is most conducive to enhancing dissolution rate (indeed, an excess of carrier promotes drug dispersion and amorphization); with this polymer, phenomena of drug recrystallization/precipitation may occur due to the low solubility of KTZ in alkaline dissolution media. Since KTZ is insoluble at $\text{pH} > 3$, the dissolution rate expectedly slowed down in phosphate buffer media. These considerations suggest that the improvement in the dissolution rate is achieved through the convergence of two factors: formulation and process.

Both polymeric proportions resulted in a higher KTZ release rate than the pure drug, as shown in Figure 6C. The release rate was significantly enhanced with a higher fraction of the polymeric carrier in the F4 co-processed system (60 % HPMCAS HF). Under these conditions, the dissolved KTZ fraction remained above 10 % for three hours. An oscillatory release behavior was observed during the first 60 minutes, possibly caused by a recrystallization/precipitation phenomenon of KTZ due to its low solubility at $\text{pH} > 3$. The graph (Figure 6D) illustrates that at a 60-minute

measurement, co-processing with 60 % HPMCAS HF resulted in the highest percentage of drug dissolution compared to pure KTZ ($p<0.0001$), physical mixture ($p=0.0004$), and the co-processed system having 33% of HPMCAS HF ($p=0.0021$). There was also a significant difference between pure KTZ and co-processed formula having 33% HPMCAS HF ($p = 0.0033$), also being the

case for the physical mixture ($p=0.0224$). Similar results were observed at 180 minutes, when 60% of HPMCAS HF co-processed systems showed significant differences compared to the rest, with the highest percentage dissolved ($p<0.0001$). For this carrier, even the physical mixture showed a significant difference compared to pure KTZ ($p=0.0457$).

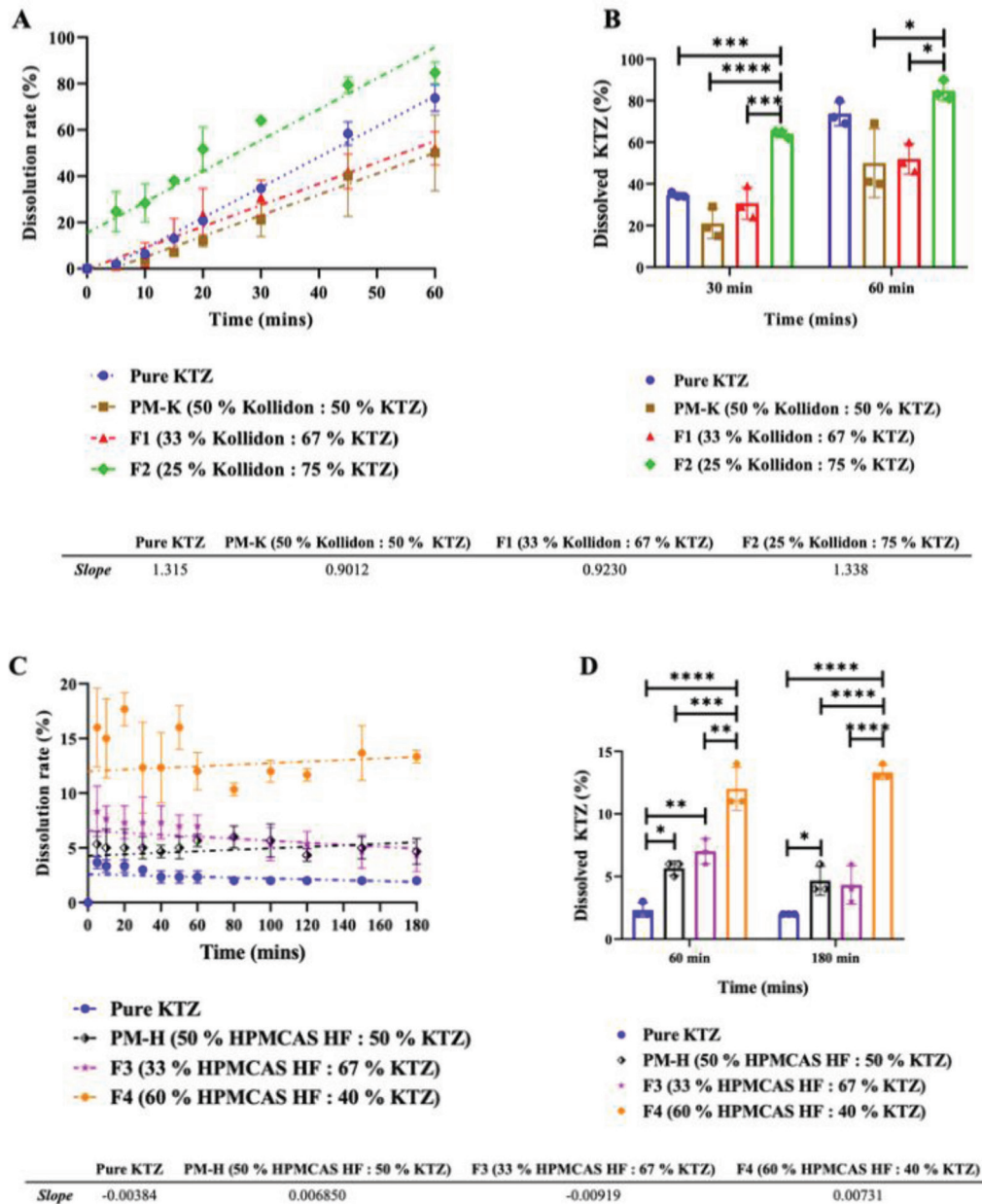


Figure 6: The dissolution rate of KTZ co-processed systems(A: Co-povidone (Kollidon™) VA 64 co-processed KTZ (25 and 33 % w/w) in 0.1 N HCl; B: Graph showing the dissolved fraction (%) at 30 and 60 minutes of the co-povidone VA 64 co-processed KTZ (25 and 33 % w/w); C: HPMCAS HF co-processed KTZ (33 and 60 % w/w) in phosphate buffer pH: 6.8; D: Graph showing the dissolved fraction (%) at 60 and 180 minutes of the HPMCAS HF co-processed KTZ (33 and 60 % w/w).

The results are presented as the mean and SEM (n=3). Linear regression, one-way ANOVA, and Tukey's multiple comparison tests were performed. * $p=0.0102$, 0.0142 , 0.0224 y 0.0457 , ** $p=0.0033$ y 0.0021 , *** $p=0.0003$, 0.0004 0.0007 , **** $p<0.0001$.

The PVP/VA-based co-povidone was more effective the more concentrated the drug was, while the HPMCAS carrier required a higher dilution of KTZ to enhance dissolution. The outcomes associated with HPMCAS are crucial for devising strategies to facilitate the direct release of drugs into the intestine. HPMCAS in HSM is a suitable strategy for designing KTZ-based formulations to be released at the intestinal site due to the drug-polymer interaction capability and the favorable pH level at which the polymer dissolves. It is expected that at a low-pH level, HPMCAS-based formulations will not release the drug during the stomach stage of the digestive process, but it will do so once the product reaches the intestine. With pH values close to 6.8, this polymeric system is activated, delivering KTZ directly at the absorption site. However, the maximum dissolved fraction of KTZ verified at pH 6.8 after 20 minutes was 19%. Through in vivo studies, it can be verified whether this result is preferable or whether co-povidone VA 64 co-processed is more suitable. Although it releases about 80% of the drug, it does so at a specific stomach pH where absorption is not verified. Therefore, it is necessary to consider the amount of drug released into the stomach medium that manages to reach the intestine while dissolved in the solubility equilibrium.

Melt granulation proves to be a valuable technique for enhancing the dissolution rate of one water-insoluble model drug. Our findings suggest that selecting the appropriate polymer is crucial in augmenting the dissolution rate and apparent solubility of poorly aqueous soluble drugs (Lee *et al.*, 2021).

4. Conclusion

Enhancing the poor solubility of effective drugs is currently a challenge for formulation scientists, so it is essential to study effective technologies that modify biopharmaceutical properties.

In this study, the co-processed F2 (25% co-povidone VA 64) significantly enhanced the dissolution rate compared to pure KTZ. Co-processing KTZ with HPMCAS (plasticized with 20% TEC) in both proportions demonstrated an increased drug dissolution rate, attributable to the reduction in the crystallinity percentage of KTZ and the ability of the system to stabilize through hydrogen bonding. These results demonstrate that MG in HSM provides a promising opportunity to develop new immediate or controlled-release

co-processed materials to be patented. If critical process parameters in HSM are controlled, efforts can be made to ensure the processes are scalable, reproducible, robust, and commercially successful.

An important objective in developing co-processed products is to optimize the amount of drug available in the body to achieve therapeutic efficacy while minimizing adverse effects. Among other advantages, this can result in the development of tablets with lower doses and smaller volumes, reducing the dosing frequency, which translates into an improvement in the quality of life for patients, but also opens an opportunity to increase the business competitiveness for the pharmaceutical industrial sector. Lower doses can drop manufacturing costs and aid in reducing the water & carbon prints in pharma-chemical plants that need high amounts of organic solvents.

Acknowledgments

The authors thank U. Hernández from the Powder X-Ray Diffraction Laboratory of the Centro Conjunto de Investigación en Química Sustentable UAEM-UNAM and A. Romo from the Instituto de Química de la Universidad Nacional Autónoma de México for their contribution to the XRPD and IR (ATR) measurements, respectively. We are very grateful to Moléculas Finas, S.A. de C.V., BASF Pharma Co. México, Ashland México, and Sigma-Aldrich México for their generous donations of some raw materials and reagents used in the study.

Authorship Contribution

Abigail Garcia-Radilla was responsible for the formal analysis, investigation, data curation, and writing of the original draft. Mariana Ortiz-Reynoso contributed to the conceptualization of the study, provided resources, curated data, and was involved in writing—review & editing, as well as supervising and acquiring funding for the project. Gabriel E. Cuevas provided essential resources, while Edna T. Alcantara-Fierro was responsible for methodology, validation, data curation, and project administration. Jonnathan G. Santillan contributed to formal analysis and writing—review & editing.

Funding

This project was funded by the Mexican Consejo Nacional de Humanidades Ciencia y Tecnología (CONAHCYT) through a national scholarship (2021-2023), and the Consejo Mexiquense de Ciencia y Tecnología (COMECyT), through the “Female Scientists” (*Mujeres Científicas*) grant awarded for the 2021 call.

Conflict of Interest

There are no conflicts of interest.

Declaration

It is original data and has neither been sent elsewhere nor published anywhere.

References

- Auch, C., Jede, C., Harms, M., Wagner, C., & Mäder, K. (2020). Impact of amorphization and GI physiology on supersaturation and precipitation of poorly soluble weakly basic drugs using a small-scale in vitro transfer model. *International Journal of Pharmaceutics*, 574, 118917. <https://doi.org/10.1016/j.ijpharm.2019.118917>
- Bouffard, J., Bertrand, F., & Chaouki, J. (2012). A multiscale model for the simulation of granulation in rotor-based equipment. *Chemical engineering science*, 81, 106-117. <https://doi.org/10.1016/j.ces.2012.06.025>
- Chan, S. Y., Chung, Y. Y., Cheah, X. Z., Tan, E. Y. L., & Quah, J. (2015). The characterization and dissolution performances of spray dried solid dispersion of ketoprofen in hydrophilic carriers. *Asian journal of pharmaceutical sciences*, 10(5), 372-385. <https://doi.org/10.1016/j.ajps.2015.04.003>
- Coksu, I., Bozkurt, Y., Akmayan, I., Demirci, H., Ozbek, T., & Acar, S. (2023). Ketoconazole-loading strategy to improve antifungal activity and overcome cytotoxicity on human renal proximal tubular epithelial cells. *Nanotechnology*, 35(11), 115702. <https://doi.org/10.1088/1361-6528/ad1444>
- Crowley, K. J., Forbes, R. T., York, P., Nyqvist, H., & Camber, O. (2000). Drug-fatty acid salt with wax-like properties employed as binder in melt granulation. *International journal of pharmaceutics*, 211(1-2), 9-17. [https://doi.org/10.1016/S0378-5173\(00\)00577-9](https://doi.org/10.1016/S0378-5173(00)00577-9)
- De Almeida, R. F., Santos, F. C., Marycz, K., Alicka, M., Krasowska, A., Suchodolski, Panek, J.J., Jezierska, A., & Starosta, R. (2019). New diphenylphosphane derivatives of ketoconazole are promising antifungal agents. *Scientific reports*, 9(1), 16214. <https://doi.org/10.1038/s41598-019-52525-7>
- Duarte Alaniz, V., Rocha-Rinza, T., & Cuevas, G. (2015). Assessment of hydrophobic interactions and their contributions through the analysis of the methane dimer. *Journal of Computational Chemistry*, 36(6), 361-375. <https://doi.org/10.1002/jcc.23798>
- European Medicines Agency (EMA). Committee for Medicinal Products for Human Use (CHMP). (2014). Public Assessment Report Ketoconazole HRA EMA/CHMP/534845/2014. *Public Assessment Report*, 44(September), 1-115. https://www.ema.europa.eu/en/documents/assessment-report/ketoconazole-hra-epar-public-assessment-report_en.pdf
- Freichel, O. L., & Lippold, B. C. (2001). An easy producible new oral hydrocolloid drug delivery system with a late burst in the release profile. *International journal of pharmaceutics*, 216(1-2), 165-169. [https://doi.org/10.1016/S0378-5173\(01\)00586-5](https://doi.org/10.1016/S0378-5173(01)00586-5)
- García, A., Ortiz, M., Alcantara, E., Santillan, J., & Hernández, F. (2024). Accelerating the development of solubility-enhanced solid dispersions: use of multiscale and mathematical prediction of drug-polymer miscibility. *European Journal of Pharmaceutical and Medical Research*, 11(2), 184-196.
- García-Radilla, A., Ortiz-Reynoso, M., Santillán-Benítez, J. G., & Alcantara-Fierro, E. T. (2023). Dispersiones sólidas de solubilidad mejorada fabricadas en mezcladores de alto corte: una oportunidad para la industria farmacéutica local mexicana. *Revista Colombiana de Ciencias Químico-Farmacéuticas*, 52(1). <https://doi.org/10.15446/rcciquifa.v52n1.102588>
- Jadav, N. B., & Paradkar, A. (2020). Solid dispersions: technologies used and future outlook. *Nanopharmaceuticals*, 91-120. <https://doi.org/10.1016/B978-0-12-817778-5.00005-1>
- Jaspers, M., Roelofs, T. P., Janssen, P. H., Meier, R., & Dickhoff, B. H. (2022). A novel approach to minimize loss of compactibility in a dry granulation process using superdisintegrants. *Powder Technology*, 408, 117773. <https://doi.org/10.1016/j.powtec.2022.117773>
- Lee, J. H., Jeong, H. S., Jeong, J. W., Koo, T. S., Kim, D. K., Cho, Y. H., & Lee, G. W. (2021). The development and optimization of hot-melt extruded amorphous solid dispersions containing Rivaroxaban in combination with polymers. *Pharmaceutics*, 13(3), 344. <https://doi.org/10.3390/pharmaceutics13030344>
- Medarević, D., Djuriš, J., Barmapalexis, P., Kachrimanis, K., & Ibrić, S. (2019). Analytical and computational methods for the estimation of drug-polymer solubility and miscibility in solid dispersions development. *Pharmaceutics*, 11(8), 372. <https://doi.org/10.3390/pharmaceutics11080372>
- Nair, A. R., Lakshman, Y. D., Anand, V. S. K., Sree, K. N., Bhat, K., & Dengale, S. J. (2020). Overview of extensively employed polymeric carriers in solid dispersion technology. *AAPS PharmSciTech*, 21, 1-20. <https://doi.org/10.1208/s12249-020-01849-z>
- Perissutti, B., Rubessa, F., Moneghini, M., & Voinovich, D. (2003). Formulation design of

carbamazepine fast-release tablets prepared by melt granulation technique. *International journal of pharmaceutics*, 256(1-2), 53-63.

[https://doi.org/10.1016/S0378-5173\(03\)00062-0](https://doi.org/10.1016/S0378-5173(03)00062-0)

Ramirez-Gualito, K., Alonso-Rios, R., Quiroz-Garcia, B., Rojas-Aguilar, A., Diaz, D., Jimenez-Barbero, J., & Cuevas, G. (2009). Enthalpic nature of the CH/ π interaction involved in the recognition of carbohydrates by aromatic compounds, confirmed by a novel interplay of NMR, calorimetry, and theoretical calculations. *Journal of the American Chemical Society*, 131(50), 18129-18138.

<https://doi.org/10.1021/ja903950t>

Rask, M. B., Knopp, M. M., Olesen, N. E., Holm, R., & Rades, T. (2016). Influence of PVP/VA copolymer composition on drug-polymer solubility. *European journal of pharmaceutical sciences*, 85, 10-17.

<https://doi.org/10.1016/j.ejps.2016.01.026>

Sarpal, K., Tower, C. W., & Munson, E. J. (2019). Investigation into intermolecular interactions and phase behavior of binary and ternary amorphous solid dispersions of ketoconazole. *Molecular Pharmaceutics*, 17(3), 787-801.

<https://doi.org/10.1021/acs.molpharmaceut.9b00970>

Singh, M., Shirazian, S., Ranade, V., Walker, G. M., & Kumar, A. (2022). Challenges and opportunities in modelling wet granulation in pharmaceutical industry—a critical review. *Powder Technology*, 403, 117380.

<https://doi.org/10.1016/j.powtec.2022.117380>

Steffens, K. E., Brenner, M. B., Hartig, M. U., Monschke, M., & Wagner, K. G. (2020). Melt granulation: a comparison of granules produced via high-shear mixing and twin-screw granulation. *International Journal of Pharmaceutics*, 591, 119941.

<https://doi.org/10.1016/j.ijpharm.2020.119941>

Tamez-Fernández, J. F., Soto-Suárez, F. M., Estrada-Chavarría, Y. D., Quijano-Quiñones, R. F., Toscano, R. A., Cuétara-Guadarrama, F., & Cuevas, G. (2021). Effect of the $nO \rightarrow \pi^* C=O$ Interaction on the Conformational Preference of 1, 3-Diketones: A Case Study of Riolozatrione Derivatives. *The Journal of Organic Chemistry*, 86(14), 9540-9551.

<https://doi.org/10.1021/acs.joc.1c00847>

Vaka, S. R. K., Bommana, M. M., Desai, D., Djordjevic, J., Phuapradit, W., & Shah, N. (2014). Excipients for amorphous solid dispersions. *Amorphous solid dispersions: Theory and practice*, 123-161.

https://doi.org/10.1007/978-1-4939-1598-9_4

Yazdani, A., Höhne, G. W., Misture, S. T., & Graeve, O. A. (2020). A method to quantify crystallinity in amorphous metal alloys: A differential scanning calorimetry study. *PloS one*, 15(6), e0234774.

<https://doi.org/10.1371/JOURNAL.PONE.0234774>

Ye, G., Wang, S., Heng, P. W. S., Chen, L., & Wang, C. (2007). Development and optimization of solid dispersion containing pellets of itraconazole prepared by high shear pelletization. *International journal of pharmaceutics*, 337(1-2), 80-87.

<https://doi.org/10.1016/j.ijpharm.2006.12.028>



CHITKARA

Journal of Pharmaceutical Technology, Research and Management

Chitkara University, Saraswati Kendra, SCO 160-161, Sector 9-C, Chandigarh, 160009, India

Volume 12, Issue 2

November 2024

ISSN 2321-2217

Copyright: [©2024 Abigail Garcia-Radilla, Mariana Ortiz-Reynoso et al.,] This is an Open Access article published in Journal of Pharmaceutical Technology, Research and Management (J. Pharm. Tech. Res. Management) by Chitkara University Publications. It is published with a Creative Commons Attribution-CC-BY 4.0 International License. This license permits unrestricted use, distribution, and reproduction in any medium, provided the original author and source are credited.